NERC Scientific Support and Facilities
Ion Microprobe Facility

University of Edinburgh
NERC Ion Microprobe Facility
2023 Annual Science Report

Ion Microprobe Facility
School of Geosciences
Grant Institute
Kings Buildings
James Hutton Road
Edinburgh
EH9 3FE

https://www.ed.ac.uk/geosciences/about/facilities/all/ionprobe

Contents

Constraining the primary sulphur concentration and isotopic composition of the Troodos ophiolite by analysis of volcanic glasses (progress report)

G. D. Bromiley[1], L. Saper[1,2], D. Woelki[3] & R. Cao[1]

[1]School of GeoSciences, University of Edinburgh, Edinburgh EH9 3FE, UK
[2]Jet Propulsion Laboratory, Pasadena, California, U.S.
[3]University of Freiburg, Freiburg, Germany

Summary of Project

We are studying a suite of (previously) well-characterised glasses from across the Troodos ophiolite, Cyprus by SIMS and X-ray Absorption Near-Edge Spectroscopy. SIMS work at Edinburgh is being performed to measure $\delta^{34}S$, H and C in the glasses, which will compliment data on S and Fe oxidation state obtained by XANES These measurements will place constraints on the primary S and $\delta^{34}S$ of Troodos melts and their mantle sources, providing new insights into (1) crust-formation processes in incipient subduction zones, and (2) the relative importance of melting, differentiation, and degassing processes in controlling volatile recycling and ore formation in supra-subduction zones.

Work conducted to date

S and Fe XANES microanalysis was conducted at beamline I3-IDE at the Advanced Photon Source (APS), Argonne National Laboratory, U.S., prior to SIMS analysis. Samples were subsequently prepared for SIMS analysis. H contents of glasses were determined using the 7f instrument at the EIMF in June 2023, although it was not possible to measure C contents at this time. Sulphur isotope analysis work will be completed in April 2023 using the 1270 instrument. Initial SIMS analysis confirmed H contents in a subset of the samples, previously determined by FTIR analysis, as described by [1], and demonstrated minimal heterogeneity within samples. We also obtained H contents in a further set of glasses obtained from Cyprus as part of this project.

Results from S and Fe XANES spectroscopy were published in a letter in Earth and Planetary Science Letters [2] in early 2024.

References

[1] Woelki, D. et al. (2019) Chemical Geology **523**, 1–8
[2] Saper, L. M. et al. (2024) Earth and Planetary Science Letters **627**, 118560

Boron isotopes trace diverse sources of boron in subducted oceanic crust

B. J. R. Harris[1], J. C. M. De Hoog[1] & R. Halama[2]

[1]School of GeoSciences, University of Edinburgh, Edinburgh EH9 3JW, UK
[2]School of Geography, Geology and the Environement, Keele University, Keele ST5 5BG, UK

Introduction

Boron is a fluid-mobile element and B isotopes are a sensitive tracer of fluid processing in subduction zones due to high B concentrations in the continental crust and seawater, strong B isotopic fractionation at the surface and low B concentration of the mantle. Arc volcanics are strongly enriched in B compared to MORB and show a significantly larger range of B isotope compositions that stretches to much higher $\delta^{11}B$ values due to the presence of seawater-derived B [1].

Altered oceanic crust (AOC) is one of the major B reservoirs in subduction zones (Fig. 1). During subduction, metamorphic recrystallisation leads to dehydration reactions during which B partitions into aqueous fluid and metasomatizes the overlying mantle wedge. As ^{11}B preferentially partitions into fluid compared to ^{10}B, these fluids remove isotopically heavy B from the subducting slab, which then becomes increasingly B depleted and isotopically light. This progressive change in B isotopic composition of the slab with depth has been used extensively in the literature to explain B isotope trends in arc volcanic rocks [2-4], as well as to explain the presence of isotopically light B in the source regions of oceanic island basalts (OIB) [5,6].

Despite this generally accepted model of B isotope composition vs slab depth, very few systematic studies of high-pressure subducted-related rocks exist to validate these models, and those that are available were restricted to show low $\delta^{11}B$ values in subduction-related rocks [7,8]. In addition, current models of slab dehydration and accompanying B isotope fractionation treat the subducting slab as a homogeneous reservoir without paying much attention to its chemical and mineralogical variability. Although fresh MORB is rather homogenous in terms of major elements, seawater alteration can change its bulk composition significantly, including 20-fold increases in K_2O content [9], an element which is very low in pristine MORB (~0.1 wt.%). This is important, as the amount of K_2O determines the modal amount of mica that forms in the rock during metamorphism, and phengite (high pressure white mica) is the main host of volatile and fluid-mobile elements including B in AOC until very high pressures and temperatures. Models that distinguished phengite-bearing vs. phengite-absent rocks showed extremely different slab compositions beneath the arc (-8 vs. -30 permil), demonstrating phengite's essential role [10], but also the need for a more accurate data of the relationship between bulk rock K_2O, phengite mode of the rock and its B isotopic composition.

Samples

We analysed 15 samples comprising greenschists, blueschists and eclogites from a range of localities including the Western Alps, Japan, Syros and the Dominican Republic. The samples were selected to represent the subducted equivalents of MORB-type basalts with varying degrees of seafloor alteration, reflected in their K_2O concentrations, ranging from <0.1 – 1.8 wt% (fresh MORB = 0.14 ± 0.01 wt%).

Results and discussion

Devolatilization would be expected to result in a positive correlation of whole rock K_2O and Ba/Nb, with mineral $\delta^{11}B$, since rocks which contain more mica (higher K_2O) will retain more B and therefore have a less negative B isotope signature. Instead there are weak negative correlations weak negative correlations between $\delta^{11}B$, and bulk rock K_2O and Ba/Nb (Figure 1). This suggests that devolatilization is not a major process controlling B isotope evolution in this suite of subducted oceanic basalts. Four samples, which are strongly enriched in K_2O (> 0.75 wt%) compared to MORB (0.14 wt%), have negative $\delta^{11}B$ values ranging from -12.3 to -2.7 permil. These samples also show correlated enrichments in K, Rb and Ba, and these features together suggest that B was primarily sourced from B-rich, sediment-derived fluids, which infiltrated the rock during subduction or exhumation.

Six samples, which are enriched in Na_2O (> 4wt %) compared to MORB (2.7 wt%), have $\delta^{11}B$ values ranging from -1.3 to +16.9 permil. They also show no geochemical evidence of interaction with either sediment-derived fluids (e.g. K-Rb-Ba enrichment) or serpentinite-derived fluids (e.g. Mg-Ni-Cr enrichment). Na-enrichment reflects spilitisation of the protolith basalts during seafloor alteration. Positive $\delta^{11}B$ values are also consistent with a seafloor alteration signature, suggesting that their B geochemistry was acquired on the seafloor and preserved during subduction and exhumation up to eclogite facies.

Together, these data demonstrate that the B isotope composition of subducted oceanic crust is much more diverse than previously suggested, and that other processes aside from devolatilization play a major role. Further work will link the record in B isotopes to that of N concentrations determined in a previous project (IMF 717/0521).

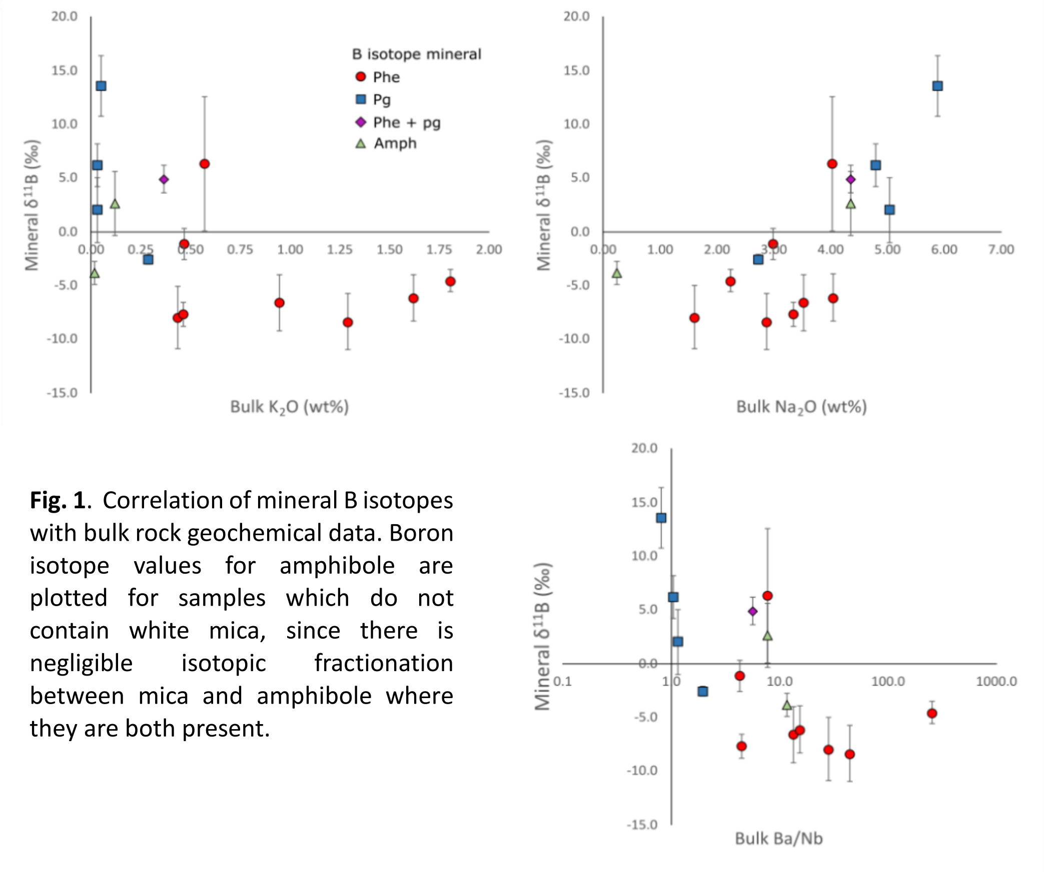

Fig. 1. Correlation of mineral B isotopes with bulk rock geochemical data. Boron isotope values for amphibole are plotted for samples which do not contain white mica, since there is negligible isotopic fractionation between mica and amphibole where they are both present.

References

[1] De Hoog, J.C.M. and I. Savov (2018) Advances in Isotope Geochemistry, Vol 9, 217-247
[2] Ishikawa & Tera (1997), EPSL **152**, 123-138
[3] Rosner et al. (2003), G3 **4** (8)
[4] Konrad-Schmolke et al., (2016), G3 **1**7, 2987-3007
[5] Hartley et al. (2021), GCA **294**, 273-294
[6] Walowski et al. (2021), GCA **30**2, 83-100
[7] Peacock and Hervig, (1999), Chem Geol **4**, 281-290
[8] King et al. (2007), Chem Geol **239**, 305-322
[9] Hacker B.R. (2008), G3 **9** (3) Q03001
[10] Marschall et al. (2007), Chem Geol **239**, 323-335

Magmatic CO_2 at Soufriere Hills Volcano, Montserrat and the importance of the vapour bubble

T. A. Howe[1], H. Tuffen[1], T. Christopher[2,3], S. Moune[4,5] & F. Schiavi[4]

[1]Lancaster Environment Centre, Lancaster University, Lancaster, LA1 4YD, UK
[2]Montserrat Volcano Observatory, Montserrat, West Indies
[3]Seismic Research Centre, University of the West Indies, Trinidad, West Indies
[4]Laboratoire Magmas et Volcans, Université Clermont Auvergne, Clermont-Ferrand, France
[5]Institut de Physique Du Globe de Paris, Université de Paris, Paris, France

Introduction

The Soufriere Hills Volcano in the Lesser Antilles began erupting in 1995 after ~400 years of dormancy. Over the last 29 years, there has been five phases of activity, marked by magma extrusion. Previous melt inclusion analysis focusing on the glass yielded <60 ppm CO_2 in quartz-hosted inclusions, and ≤1032 ppm CO_2 for plagioclase and orthopyroxene hosted inclusions[1,2]. Solubility models using combined CO_2 and H_2O concentrations have estimated equilibrium pressures of 100 – 300 MPa, equivalent to ~5-6 km depth. However, a two-level magmatic system is proposed for Soufriere Hills Volcano, based on geochemical and geophysical studies, linking previous melt inclusion data to the upper storage level.

Recent studies of CO_2 in melt inclusions reveal that up to ≥90% of CO_2 is sequestered to the bubble during post-entrapment modification[3,4]. As a consequence, analysis of melt inclusions neglecting the bubble can severely underestimate the total CO_2, and therefore underestimates magma storage depths.

To investigate the effect of the unmeasured CO_2 in Soufriere Hills Volcano melt inclusion bubbles in previous studies, CO_2 and H_2O were analysed in the glass of plagioclase and orthopyroxene melt inclusions via SIMS along with S, Cl and F for further understanding of volatile systematics, and CO_2 was also analysed in the bubble via Raman spectroscopy.

Results

Melt inclusions from four phases of eruptive activity range from 83 – 2800 ppm CO_2 and 2.47 – 7.26 wt% H_2O (Fig. 1) total. In the glass, CO_2 ranges from 13 – 1243 ppm, similar to previous Soufriere Hills Volcano studies. Additionally, CO_2 in the bubble at Soufriere Hills Volcano range from 13 – 2769 ppm. This indicates that an overall 6 – 99% of CO_2 is held in the bubble (Fig 2.). Estimating entrapment pressures and depths using total CO_2 and H_2O and the solubility model MagmaSat, depths inferred using bubble + glass CO_2 are up to 7 km deeper compared to glass only CO_2 and previously published melt inclusion work for Soufriere Hills Volcano.

There are some intriguing and systematic changes in bubble H_2O and CO_2 from one eruptive phase to the next (Fig. 1), with an overall decrease in magmatic H_2O from phases 1-4, followed by a strong increase in the most recent phase 5. The CO_2 concentrations are broadly similar in all phases with the exception of phase 1, which lacks the highest values, but together with high H_2O are indicative of some of the deepest magma storage conditions.

The next steps, which are already underway, are to relate to potential ranges of magma storage depths, and to integrate these insights with additional information, e.g. from deformation models, depths of recorded seismicity, gas chemistry, and petrological constraints, to create a revised and holistic model of SHV magma storage conditions. This will lead to a publication.

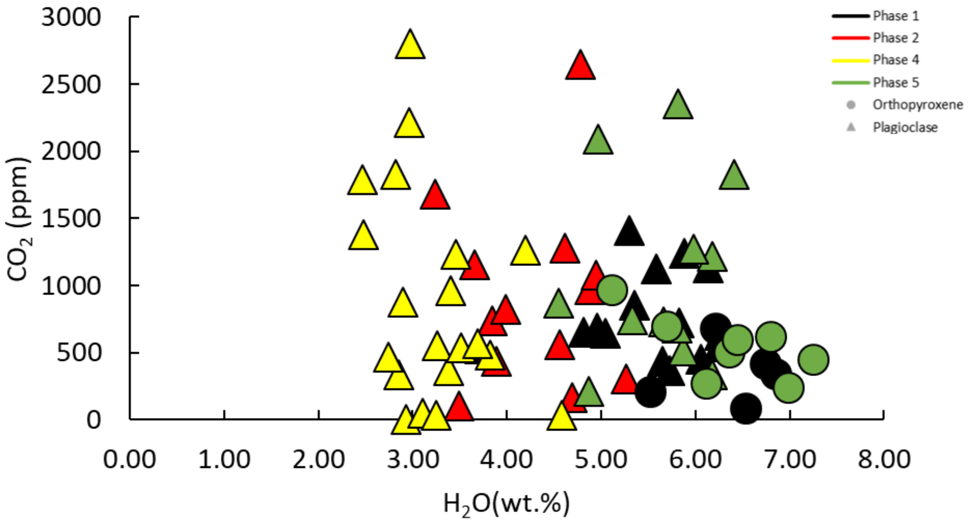

Fig. 1. Total CO_2 (glass and bubble) and H_2O contents of plag- and opx-hosted melt inclusions from Soufriere Hills Volcano, Montserrat.

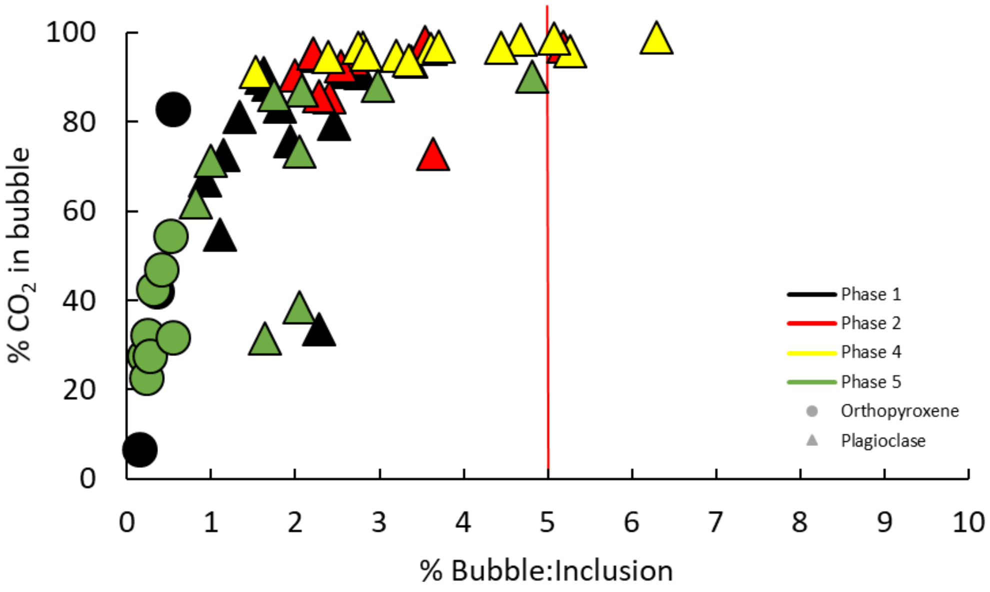

Fig. 2. Percentage of CO_2 in bubble vs bubble-inclusions ratio. For plagioclase hosted inclusions, 31 – 99% of CO_2 is contained in the bubble, and for orthopyroxene hosted inclusions, 6 – 83% of CO_2 is contained in the bubble.

References

[1] J. Barclay et al., (1998) Geophysical Research Letters **25,** 3437-3440
[2] M. Edmonds et al., (2014) Geological Society, London, Memoirs, **39**, 291–315
[3] M. Hartley et al., (2014) Earth and Planetary Science Letter, **393**, 120-131
[4] Moore et al., 2015 (2015) American Mineralogist, **100,** 806-823

What controls magma chemistry at arc settings?

E. Melekhova, B. Morrison Evans & J. Blundy

Department of Earth Sciences, University of Oxford, Oxford, OX1 3AN, UK

Introduction

This report combines two studies on basaltic andesite magmas from Kluchevskoy volcano, Kamchatka volcanic arc, Russia, and St Vincent volcano, Lesser Antilles volcanic arc, Eastern Caribbean.

Over the last couple of decades our understanding of magmatic architecture of volcanic system shifted from big magma chambers to extensive, crystal-rich, 'mushy' systems. This conceptual change brought new questions including the perception of the dominant processes controlling chemical evolution of magma. Many long-lived volcanic systems erupt a limited range of magmas over almost their entire eruptive history. Kluchevskoy and St Vincent are good examples of volcanic system that predominantly generated only basaltic andesite lavas. In this study we tested a hypothesis that melt composition is controlled by multiply-saturated mineral assemblages in the magma source region. We found that slight differences in the basaltic andesite composition and the tectonic settings leads to Kluchevskoy basaltic andesite being primary mantle derived magma and basaltic andesite from St Vincent is differentiated product of high-MgO basalt and originated at mid-crustal conditions.

Kluchevskoy basaltic andesite magmas

Primary magmas in volcanic arcs exhibit wide compositional diversity on both local and global scales. Processes responsible for this diversity are generally ascribed to some combination of mantle melting or crustal differentiation processes. One widespread view is that arc magmagenesis is driven by some combination of H_2O-fluxed and decompression melting of peridotitic mantle wedge, and that primary, mantle-derived melts are high-MgO basalt. However, a variety of other mantle-derived primitive arc magmas, ranging in composition from high-Mg andesite to picrite, has been recognised and it remains unclear to what extent this diversity can be generated by mantle melting processes modulated, for example, by changes in the thermal state of the mantle wedge or the supply of fluid from the slab. Here we use high pressure and temperature experiments to constrain magma generation conditions of a primitive magnesian (8.8 wt% MgO) basaltic andesite from Klyuchevskoy, Kamchatka arc, Russia. We use an inverse experimental approach to define a multiple saturation point on the liquidus surface of the basaltic andesite. The experimental multiple saturation point defines the pressure and temperature at which an erupted melt could have last been in equilibrium with a polymineralic source rock, such as mantle peridotite, and hence provides a robust estimate of magma source conditions.

Equilibrium piston-cylinder experiments were carried out between 0.5 and 1.0 GPa under hydrous conditions (3 to 6 wt% added H_2O) at $fO_2 = \Delta NNO+1$. We show that Klyuchevskoy basaltic andesite is multiply saturated with the lherzolite assemblage ol (Fo_{90}) + clinopyroxene + orthopyroxene + Cr-spinel close to its liquidus (≥ 95% melt) in the pressure range of 0.6 to 1 GPa (23 to 36 km depth) and 1220-1240 °C (Fig1). Amphibole is present at temperatures just below the multiple saturation point (≤1200 °C). These results show that basaltic andesite was produced by 8 to 11 wt% partial melting of amphibole-lherzolite source and therefore represents a primary, undifferentiated magma extracted from its source at near-Moho depths. These results are in a good agreement with geophysical studies of Klyuchevskoy that show magmas are supplied directly from a reservoir at near-Moho depths (25-30 km) through a sub-vertical, pipe-like feeder system (Fig. 1). Coeval high-MgO basalts from Klyuchevskoy may correspond to higher degree mantle melts extracted at slightly greater depths.

Our results provide a tight constraint on the thermal structure of the mantle wedge beneath Klyuchevskoy. Experimental temperatures are higher than those calculated from steady-state thermal models suggesting that upwelling asthenosphere might directly impinge the Moho in a similar fashion to mid-ocean ridges. Intra-arc rifting promotes asthenospheric decompression beneath the Central Kamchatka Depression. The presence of amphibole in our experiments at temperatures up to 1200 °C indicates that dehydration melting of amphibole peridotite formed by metasomatism of mantle wedge by slab-derived fluids is the primary magma generating process. Integrating our results with published multiple-saturation experiments we show that Klyuchevskoy basaltic andesite is one of a family of primary arc magmas whose compositions depend on mantle wedge thermal structure and H_2O activity. Amphibole stability exercises an important control on melting conditions.

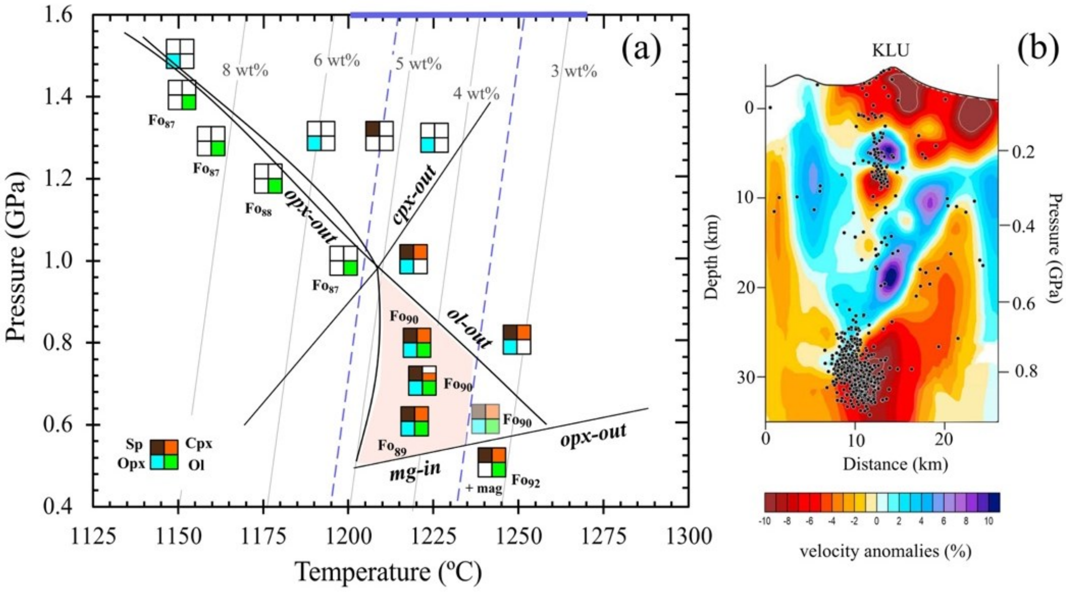

Fig. 1. (a) Liquidus surface diagram for high-MgO basaltic andesite (KLU-96-03) used to define the liquidus multiple saturation point. Only experiments with ≥ 90% glass are plotted. Olivine composition (mole% Fo) shown next to experimental symbols. Liquidus contours (dashed grey lines) are labelled with the corresponding H_2O content of the melt. The pink shaded area is the region of last equilibration of KLU-96-03 with mantle lherzolite. It was defined by two olivine-out and two pyroxene-out curves. The water content range of melt inclusions and eruptive temperature of high-MgO basaltic andesite lavas of Kluchevskoy volcano are shown by the blue bar and dashed lines respectively. Liquidus experiments on high MgO-basaltic andesite (JR-28; Table 1) from Volcano Jorullo, Mexico [1] at pressures ≥1 GPa are plotted to constrain phase stability at high pressures. **(b)** Tomographic image, adapted from [2], showing S-wave velocity anomalies beneath Klyuchevskoy volcano (KLU). The black dots are earthquakes. Note the agreement between the location of deep earthquakes (22-35 km) and experimentally determent last equilibration of KLU-96-03 with lherzolite (23-36 km; 0.6 to 1 GPa) in (a). The cluster of earthquakes at ~9 km depth is attributed to degassing and associated crystallisation.

St Vincent basaltic andesite magmas

La Soufrière volcano, St Vincent (Eastern Caribbean), has throughout its lifetime produced predominantly basaltic andesite magmas, including most recently in 2020-21. We explore the origin and phase relations of these erupted magmas by performing a series of near-liquidus, high-pressure, high-temperature experiments. Melt extracted from a mush will be multiply-saturated on its liquidus with the mush mineral assemblage at the P-T-fO_2-XH_2O conditions at the time of segregation. In a system with relatively low thermodynamic variance, for example, five or six independent chemical components (as determined by principal component analysis), many coexisting mineral phases (e.g. plag+cpx+amph+oxides) and a well-constrained fO_2, multiple saturation can be reduced to an invariant point on the liquidus of the melt in P-T-H_2O space. The approach of finding liquidus multiply saturation for igneous rocks offers a novel magma source thermobarometer and hygrometer.

Equilibrium experiments using basaltic andesite magma from La Soufrière, St Vincent have been performed at 0.2-0.9 GPa, at temperatures ranging between 980-1180 °C, fO_2 ~ Ni-NiO, and with H_2O contents of 2-8 wt. %. Plagioclase, clinopyroxene and Fe-Ti oxides are found to be ubiquitous in the melt source region. Orthopyroxene is found to be more stable at higher pressures and ilmenite at lower temperatures. Amphibole is found in one equilibrium experiment. A series of slow cooling experiments find amphibole to grow extensively on the rim of clinopyroxene crystals, at lower temperatures and higher water contents. This peritectic reaction involving amphibole is also observed in St Vincent xenoliths and could signify temperature fluctuations and fluid mobility in the mush. Five-phase multiple saturation at the liquidus (melt fraction ≥ 85 %) is found for melt H_2O contents of 8 wt. %, at 0.6 GPa pressure (~22 km depth) and temperatures of 1030-1050 °C (Fig. 2). The saturating assemblage is a hornblende gabbro (cpx+plag+amph+Fe-Ti oxides) consistent with the mineralogy of plutonic xenoliths from historic eruptions of St Vincent. Mineral compositions in these multiply-saturated runs (calcic plagioclase An75-85 and high Mg # clinopyroxene) are similar to those in the xenoliths. Temperatures agree with mineral geothermometry estimates for the 2020-21 eruption, suggesting little cooling of the magma during ascent from its source region. Seismicity prior to the 2020-21 eruption is also consistent with mid-crustal source depths. Magmas sourced from similar depths can account for the limited compositional diversity of La Soufrière over its volcanic history (Fig. 2).

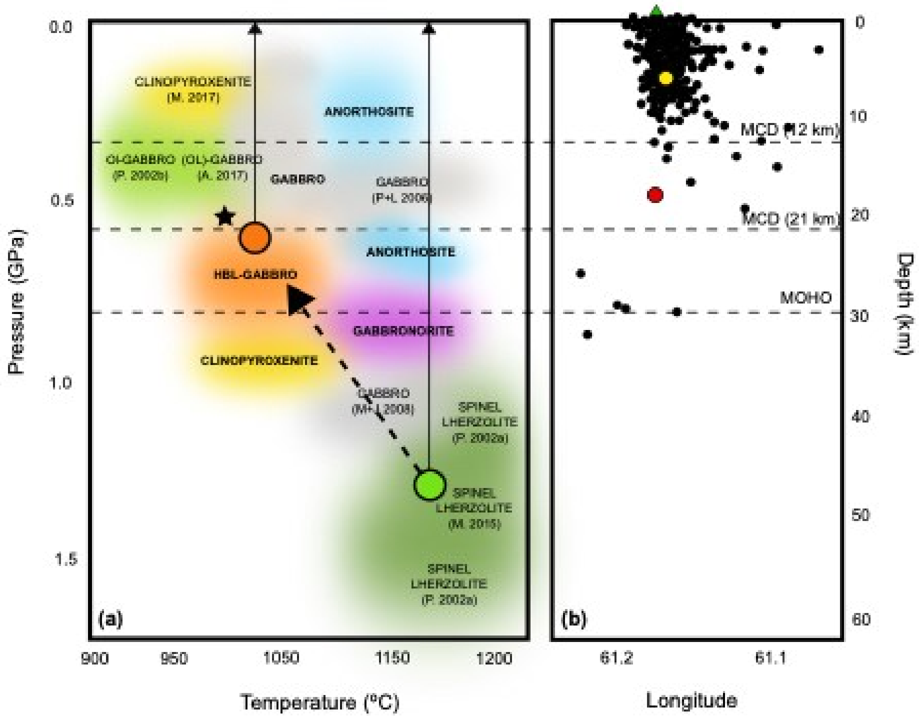

Fig. 2. Crustal structure beneath La Soufrière, St Vincent determined using experiments, petrology and geophysics. Dashed lines show estimated mid-crustal discontinuities (MCD) at 12 and 21 km and the Moho at 29 km depth [3]. (a) Near-liquidus crustal assemblages shown as corresponding xenolith compositions in pressure and temperature space. Orange circle represents experimental source depth of 2021 La Soufrière basaltic andesite melt. Green circle represents experimental source depth of high MgO basalts from St Vincent in equilibrium with a spinel lherzolite assemblage [3,4]. Black star denotes estimated source depth of 2021 La Soufrière basaltic andesite melt using MagMaTaB thermobarometer [5]. Bold xenolith names depict near liquidus experimental runs. Other near liquidus assemblages are from experiments with similar basaltic andesite starting materials (b) Black circles show earthquake foci from the 2020-21 eruption. Red and yellow circles show the modelled pre- and syn- eruptive source depths at 18 and 6 km, respectively [6,7].

References

[1] Weaver et al. (2011) Contributions to Mineralogy and Petrology **166**, 825-843
[2] Koulakov et al. (2017) Journal of Geophysical Research: Solid Earth **122** (5), 3852-3874
[3] Melekhova et al. (2019) Earth and Planetary Science Letters **516**, 12-24
[4] Pichavant et al. (2002) Geochimica et Cosmochimica Acta **66**, 2193-2209
[5] Melekhova et al. (2015) Journal of Petrology **56** (1), 161-192
[6] Weber and Blundy (2024) Geological Society, London, Special Publications **539** (1), 171-200
[7] Joseph et al. (2022) Nature Communications **13** (2022): 4129
[8] Camejo-Harry et al. (2024) Geological Society, London, Special Publications **539** (1), 41-62

A comparison of apatite and melt inclusion compositions as tracers of magmatic volatile evolution

G. Stonadge[1], A. Miles[1] & D. Smith[1]

[1]School of Geography Geology and the Environment, University of Leicester, Leicester, UK, LE1 7RH

Introduction

Apatite is a promising tool for studying magmatic volatiles (F, Cl, OH, S) in lithologies where melt inclusions (MIs) are rare or affected by post-entrapment processes (e.g., crystallisation, bubble growth and diffusion). However, well preserved MIs may still retain information about magma storage conditions and the compositional evolution of magmas, particularly towards the latter stages of crystallisation [1]. When coupled, apatite and MIs provide a potentially powerful way of either cross-referencing, or providing a more detailed history of volatile behaviour.

In this study, the composition of melt and apatite inclusions from in pumices from two volcanoes - Taal and Mt. Pinatubo - were quantified by SIMS. These two volcanic systems show contrasting H_2O saturation behaviours [2], appropriate for testing the ability for apatite and MI records to inform on differing volatile systematics. Using volatile and trace element models, we compared these two archives at both volcanoes. We analysed ^{1}H, ^{12}C, ^{19}F, ^{23}Na, ^{26}Mg, ^{30}Si, ^{32}S, ^{35}Cl, ^{39}Mn, ^{57}Fe, ^{27}Al, ^{30}Si, ^{42}Ca, ^{88}Sr, ^{89}Y, ^{140}Ce, ^{141}Pr, ^{149}Sm, ^{153}Eu, and ^{232}Th by SIMS. Apatite compositions were converted to melt compositions for comparison with MI data. Volatile mole fraction (X) ratios were calculated using the thermodynamic model of [3], and trace element melt compositions were calculated using experimentally defined partition coefficents [4].

Results & discussion

Apatites and MIs displayed variations in trace and volatile element composition (Figs. 1&2). Significantly, the relationship between the trace elements and volatiles in MIs is similar at both Taal and Pinatubo (Figs. 1&2), where F and Cl decrease slightly with decreasing Sr (used here as a proxy for increasing crystallisation). By contrast, apatites record different relationships between their trace element and volatile constituents at both volcanoes (Fig. 2). As Y increases during crystallisation, X_F/X_{Cl} increases within Pinatubo magmas whilst X_{Cl}/X_{OH} and X_F/X_{OH} decrease. By contrast, at Taal, X_F/X_{Cl} decreases whilst X_{Cl}/X_{OH} increases during crystallisation (Fig. 2)

Using trace and volatile element models, we investigated the processes recorded by the apatite and MIs at both volcanic systems. Our modelling approach used a similar method to that of [2] but was adapted to include trace elements.

Fluid-saturated crystallisation models replicated the trends in F, Cl and Sr from MIs in both volcanic systems (Fig. 1). It is likely that decreases in Cl reflect its partitioning into an exsolved fluid during crystallisation due to its low crystal compatibility (Kd << 1) and significant degree of fluid-partitioning within compositionally evolved melts [3].

At Pinatubo, decreasing X_{Cl}/X_{OH} and increasing X_F/X_{Cl} in apatite during crystallisation are best explained by fluid-saturated crystallisation [1]. This is because fluid partitioning of Cl leads to a decrease relative to F (which is fluid incompatible) and OH (which is buffered during saturated crystallisation [1,2]). By contrast, calculated melt compositions from apatites from Taal show a decrease in melt X_F/X_{Cl} and increase in X_{Cl}/X_{OH} during crystallisation (Fig. 2). Such trends were best replicated with fluid-undersaturated crystallisation models, where Cl increases in the melt relative to F and OH because of its highly incompatible behaviour in crystal phases, and the absence of open system degassing [3].

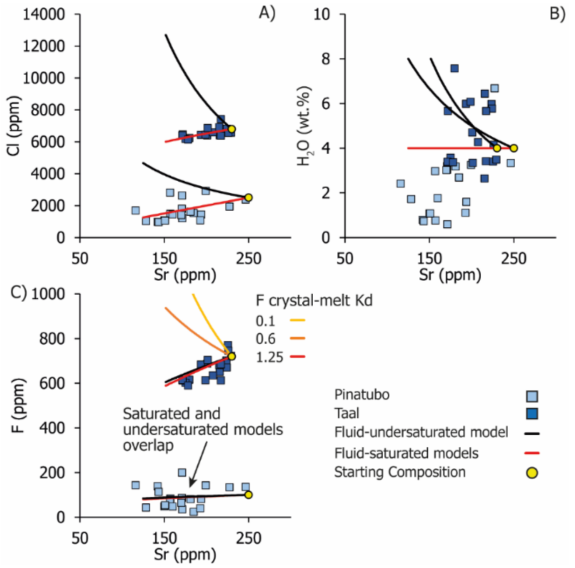

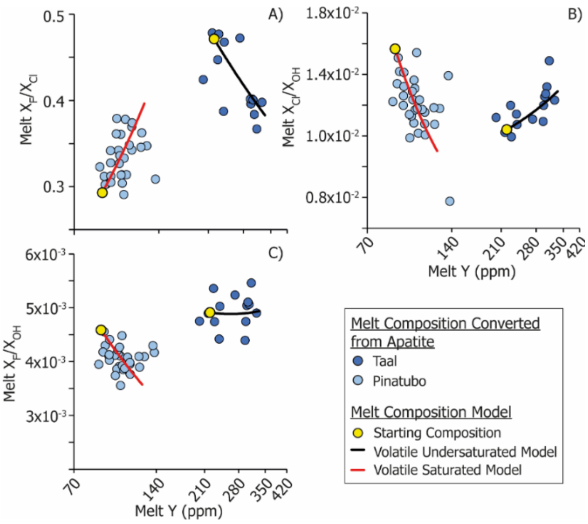

Fig. 1. (A-C) Crystallisation models of MI volatile and Sr composition. Lines on the graphs represent the predicted evolution of melt composition during fluid-saturated and fluid-undersaturated crystallisation. Melt composition models represent a total crystallisation of 50%. All data were collected by SIMS.

Fig. 2. (A-C) Melt volatile and trace element composition calculated from apatite. Lines on the graphs represent the evolution of melt chemistry during fluid-saturated and fluid-undersaturated crystallisation. Melt volatile composition is displayed as mole fraction (X) ratios. The crystallisation models represent a total of 30% crystallisation at Pinatubo and 45% at Taal.

Summary and Implications

At Pinatubo, MI compositions complement that of apatite inclusions and document a similar record of fluid-saturated crystallisation. By contrast, MIs from Taal document a different volatile record to that of apatites from the same sample. We suggest that Taal apatites formed from less evolved and fluid-undersaturated melts, while MIs reflect more evolved and later-stage, fluid-saturated conditions. Where MIs and apatites form contemporaneously, both archives provide a correlative record of fluid-saturation. By contrast, where MIs and apatite are not coeval (as seen at Taal), they may be able to record a more protracted period of magma crystallisation, characterised by changing volatile behaviours over time. Due to the heightened risk of diffusion and post entrapment modification in MIs, we suggest that apatite is a more reliable tool for studying volatile systematics in the protracted history of plutonic systems where the understanding of volatile behaviour is paramount (e.g., porphyry copper systems).

References

[1] M.C. Humphreys et al. (2021) Earth and Planetary Science Letters **576**, 117-198
[2] G.R. Stonadge et al. (2023) Geology **51** (12), 1158–1162
[3] A.A. Iveson et al. (2017) Journal of Petrology **58**, 2465-2492
[4] W. Li and F. Costa (2020) Geochimica et Cosmochimica Acta **269**, 203-222
[5] S. Prowatke and S. Klemme (2006) Geochimica et Cosmochimica Acta **70**, 4513-4527